Eur. Phys. J. B **48**, 339–348 (2005)
DOI: 10.1140/epjb/e2005-00406-x

THE EUROPEAN PHYSICAL JOURNAL B

Mott transition in the asymmetric Hubbard model at half-filling within dynamical mean-field theory

I.V. Stasyuk and O.B. Hera[a]

Institute for Condensed Matter Physics of the National Academy of Sciences of Ukraine, 1 Svientsitskii Str., 79011 Lviv, Ukraine

Received 12 April 2005 / Received in final form 22 October 2005
Published online 23 December 2005 –

Abstract. The asymmetric Hubbard model with hopping integrals dependent on an electron spin (particle sort) is studied using an approximate analytic method within the dynamical mean-field theory. The equations of motion for Hubbard operators followed by projecting and different-time decoupling are used for solving the single-site problem. Particle spectra are investigated at half-filling within various approximations (Hubbard-I, alloy-analogy and a generalization of the Hubbard-III approximation). At half-filling these approximations can describe only continuous gap opening in the spectrum. The approach is used to describe the system between two limit cases (the Falicov-Kimball model and the standard Hubbard model) with continuous transition where U_c is dependent on the value of hopping parameters of different particles.

PACS. 71.10.Fd Lattice fermion models (Hubbard model, etc.) – 71.27.+a Strongly correlated electron systems; heavy fermions – 71.30.+h Metal-insulator transitions and other electronic transitions

1 Introduction

The asymmetric Hubbard model is considered as a generalization of the Falicov-Kimball model [1] and the Hubbard model [2]. This model describes a system with two sorts of mobile particles (ions, electrons or quasiparticles) with different hopping integrals and different values of chemical potentials.

The hopping of particles is described by creation and annihilation operators and transfer parameters t_{ij}^{σ}. The Hamiltonian of the model is

$$H = \sum_i H_i + \sum_{ij\sigma} t_{ij}^{\sigma} a_{i\sigma}^{\dagger} a_{j\sigma}, \tag{1}$$

where the singe-site part

$$H_i = -\sum_{\sigma} \mu_{\sigma} n_{i\sigma} + U n_{i\uparrow} n_{i\downarrow} \tag{2}$$

includes chemical potentials μ_{σ} and a local on-site repulsion U ($n_{i\sigma} = a_{i\sigma}^{\dagger} a_{i\sigma}$). Such a Hamiltonian was considered in investigating mixed-valence compounds as an extension of the Falicov-Kimball model [3,4] introducing finite nonzero hopping integrals of localized particles ($f-f$ hopping). Also, this model can be applied to ionic conductors with two types of ions.

Due to a complexity of the problem the asymmetric Hubbard model is much less investigated than its limiting cases: the Falicov-Kimball and Hubbard models. The model was investigated in the large U limit at half-filling. The effective Hamiltonian corresponding to the anisotropic Heisenberg model was derived [3,5] and the effective antiferromagnetic interaction was discussed [4,6]. A phase separation phenomenon was considered in the ground state of the asymmetric Hubbard model [7]. Some progress has been achieved in the case of one-dimensional chains [8,9].

Essential achievement in the theory of the strongly correlated electron systems is connected with the development of the dynamical mean-field theory (DMFT) proposed by Metzner and Vollhardt [10] for the Hubbard model (see also Ref. [11] for a review). This method is based on the assumption that the self-energy is a pure local (single-site) quantity $\Sigma_{ij}^{\sigma}(\omega) = \Sigma^{\sigma}(\omega)\delta_{ij}$ and it becomes exact in the limit of infinite dimensions [12]. The current growing interest to DMFT is related to a new developing technique combining DMFT and the density functional theory within the local density approximation (LDA). The new approach LDA+DMFT [13] allows one to calculate the electronic structure of real materials correctly taking into account the strong local correlations (see Refs. [14,15] for reviews).

The Falicov-Kimball and Hubbard models were intensively investigated within DMFT (see reviews [11,16]). In the Falicov-Kimball model, particle densities of states can

[a] e-mail: hera@icmp.lviv.ua

be calculated exactly [17–22]. However, the spectrum of localized particles was investigated mostly at half-filling. In the case of the half-filled Hubbard model, a number of numerical and analytic approximate methods was developed and applied to the investigation of metal-insulator transitions [23–34].

We use an approximate analytic approach to the investigation of the band structure of the asymmetric Hubbard model in DMFT [35]. This method was developed for the Hubbard model [36,37] and it is based on a mapping of the problem onto the effective single-site Hamiltonian with auxiliary Fermi-operators describing the environment of a given site. The approach is based on equations of motion for Hubbard operators followed by the different time decoupling of the higher order Green's functions. The irreducible parts are separated off using projecting on the basis of fermionic Hubbard operators. This approach gives DMFT equations in the approximation that is a generalization of the Hubbard-III approximation and includes as simple specific cases the modified alloy-analogy approximation [38] and the Hubbard-III approximation [39]. We call it the generalized Hubbard-III (GH3) approximation. Recently, an alternative decoupling scheme in an equation of motion approach to the Hubbard model in infinite dimensions has been proposed in reference [40].

This paper is organized as follows. In Section 2, we review the formalism of DMFT, where particle hopping can be introduced in two different ways: using the coherent potential or the effective single-site Hamiltonian with the auxiliary Fermi-filed [36]. The equation of motion approach with the projecting technique and the different-time decoupling scheme is described in Section 3. This approach gives the DMFT equations within the generalized Hubbard-III approximation. In Section 4, simpler approximations to the asymmetric Hubbard model are introduced. In Section 5, some analytic properties concerning continuous metal-insulator transitions are derived. Our results are discussed in Section 6, and concluding remarks are given in Section 7.

2 Dynamical mean field theory

The particle Green's function in the Matsubara representation is defined as follows

$$G_{ij}^{\sigma}(\tau-\tau') = \langle \mathcal{T}_\tau a_{i\sigma}^{\dagger}(\tau) a_{j\sigma}(\tau')\rangle, \tag{3}$$

$$G_{ij}^{\sigma}(\omega_n) = \int_0^\beta G_{ij}^{\sigma}(\tau) \mathrm{e}^{-\mathrm{i}\omega_n\tau}\mathrm{d}\tau, \quad \omega_n = \frac{\pi(2n+1)}{\beta}, \tag{4}$$

where $\mathcal{T}_\tau$ denotes imaginary time ordering, and $\beta = 1/T$ is the inverse temperature.

If we consider a perturbation expansion in terms of hopping (t_σ) instead of the interaction U, the particle Green's function can be written as a solution of the Larkin equation [41,42]:

$$G_{ij}^{\sigma}(\omega_n) = \Xi_{ij\sigma}(\omega_n) + \sum_{lm} \Xi_{il\sigma}(\omega_n) t_{lm}^{\sigma} G_{mj}^{\sigma}(\omega_n), \tag{5}$$

or in momentum space

$$G_\sigma(\omega_n,\mathbf{k}) = \Xi_\sigma(\omega_n,\mathbf{k}) + \Xi_\sigma(\omega_n,\mathbf{k}) t_{\mathbf{k}}^{\sigma} G_\sigma(\omega_n,\mathbf{k}), \tag{6}$$

where $\Xi_\sigma(\omega_n,\mathbf{k})$ is the total irreducible part (also called irreducible cumulant) that cannot be divided into parts by cutting one hopping line. It is connected to the Dyson self-energy by the relation [11]:

$$\Xi_\sigma^{-1}(\omega_n,\mathbf{k}) = \mathrm{i}\omega_n + \mu_\sigma - \Sigma_\sigma(\omega_n,\mathbf{k}). \tag{7}$$

In the limit of high lattice dimensions $d \to \infty$, the irreducible part becomes a single-site quantity [12,43]:

$$\Xi_{ij\sigma}(\omega_n) = \Xi_\sigma \delta_{ij}, \quad \Xi_\sigma(\omega_n,\mathbf{k}) = \Xi_\sigma(\omega_n). \tag{8}$$

The function $\Xi_\sigma(\omega_n)$ or $\Sigma_\sigma(\omega_n)$ is calculated using the auxiliary single-site problem. This problem corresponds to the following replacement

$$\mathrm{e}^{-\beta H} \to \mathrm{e}^{-\beta H_{\mathrm{eff}}} = \mathrm{e}^{-\beta H_0} \mathcal{T}_\tau \exp\left[-\int_0^\beta \mathrm{d}\tau H_{\mathrm{int}}(\tau)\right], \tag{9}$$

$$H_{\mathrm{int}}(\tau) = \int_0^\beta \mathrm{d}\tau' \sum_\sigma J_\sigma(\tau-\tau') a_\sigma^{\dagger}(\tau) a_\sigma(\tau'), \tag{10}$$

where

$$H_0 = H_i, \tag{11}$$

and $J_\sigma(\tau-\tau')$ is the coherent potential. This function describes the propagation of a particle in the environment without going through the given site between moments τ and τ'. It is determined self-consistently from the condition that the same irreducible part determines the lattice single-site Green's function

$$G_\sigma(\omega_n) = G_{ii}^{\sigma}(\omega_n) = \frac{1}{N}\sum_{\mathbf{k}} G^{\sigma}(\omega_n,\mathbf{k}), \tag{12}$$

$$G_\sigma(\omega_n,\mathbf{k}) = \frac{1}{\Xi_\sigma^{-1}(\omega_n) - t_{\mathbf{k}}^{\sigma}} \tag{13}$$

and the Green's function of the effective single-site problem

$$G_\sigma(\omega_n) = \frac{1}{\Xi_\sigma^{-1}(\omega_n) - J_\sigma(\omega_n)}. \tag{14}$$

To investigate the Green's functions in the time representation the analytic continuation from the imaginary to real axis ($\mathrm{i}\omega_n \to \omega + \mathrm{i}\varepsilon$) is performed:

$$G_\sigma(\omega_n) \to G_\sigma(\omega) = 2\pi\langle\langle a_\sigma | a_\sigma^{\dagger}\rangle\rangle_\omega, \tag{15}$$

$$\Xi_\sigma(\omega_n) \to \Xi_\sigma(\omega), \quad J_\sigma(\omega_n) \to J_\sigma(\omega). \tag{16}$$

The self-consistency condition is rewritten in the following form

$$G_\sigma(\omega) = \int_{-\infty}^{+\infty} \frac{\rho_\sigma^0(t)\mathrm{d}t}{\Xi_\sigma^{-1}(\omega) - t}, \tag{17}$$

where (13) is inserted into (12) and the sum over $\mathbf{k}$ is replaced by the integration with the noninteracting density of states.

A solution of the single-site problem (9) gives the particle Green's function $G_\sigma(\omega)$ as a functional of the coherent potential $J_\sigma(\omega)$. This dependence supplemented by the self-consistency condition forms a closed set of equations for the single-site Green's function and the coherent potential.

We reformulate the single-site problem introducing an effective Hamiltonian as it was done in reference [36]:

$$H_{\rm eff} = H_0 + \sum_\sigma V_\sigma \big(a_\sigma^\dagger \xi_\sigma + \xi_\sigma^\dagger a_\sigma\big) + H_\xi. \tag{18}$$

The auxiliary fermionic operators $\xi_\sigma^\dagger$, ξ_σ are introduced to describe particle hopping between the site (H_0) and effective environment defined by the Hamiltonian H_ξ. The coherent potential is expressed as a Green's function in the unperturbed Hamiltonian H_ξ:

$$J_\sigma(\omega) = 2\pi V_\sigma^2 \langle\langle \xi_\sigma | \xi_\sigma^\dagger \rangle\rangle_\omega^\xi. \tag{19}$$

Thus, an explicit form of H_ξ is not required to solve the problem.

3 Generalized Hubbard-III approximation

We use the single-site Hamiltonian of the asymmetric Hubbard model written in terms of Hubbard operators

$$H_0 = -\sum_\sigma \big[\mu_\sigma \big(X^{\sigma\sigma} + X^{22}\big)\big] + UX^{22}, \tag{20}$$

acting on the basis of single-site states $|n_A, n_B\rangle$

$$\begin{array}{ll} |0\rangle = |0,0\rangle, & |A\rangle = |1,0\rangle, \\ |2\rangle = |1,1\rangle, & |B\rangle = |0,1\rangle. \end{array} \tag{21}$$

In this case, the particle creation and annihilation operators are expressed as

$$a_\sigma = X^{0\sigma} + \zeta X^{\bar\sigma 2}, \tag{22}$$

and the two-time Green's function $G_\sigma(\omega) \equiv 2\pi\langle\langle a_\sigma | a_\sigma^\dagger\rangle\rangle_\omega$ is expressed as:

$$\begin{aligned} G_\sigma = 2\pi\big[&\langle\langle X^{0\sigma}|X^{\sigma 0}\rangle\rangle_\omega + \zeta\langle\langle X^{0\sigma}|X^{2\bar\sigma}\rangle\rangle_\omega \\ &+ \zeta\langle\langle X^{\bar\sigma 2}|X^{\sigma 0}\rangle\rangle_\omega + \langle\langle X^{\bar\sigma 2}|X^{2\bar\sigma}\rangle\rangle_\omega\big], \end{aligned} \tag{23}$$

where the following notations for sort indices are used: $\bar\sigma = B$, $\zeta = +$ for $\sigma = A$ and $\bar\sigma = A$, $\zeta = -$ for $\sigma = B$.

To calculate the Green's functions $\langle\langle X^{0\sigma(\bar\sigma 2)} | X^{\sigma 0(2\bar\sigma)}\rangle\rangle$, we use the procedure described in details in [35,44]. The equations of motion for Hubbard operators are used, where the commutators are projected on the subspace formed by fermionic operators $X^{0\sigma}$ and $X^{\bar\sigma 2}$:

$$\big[X^\gamma, H_{\rm eff}\big] = \alpha_1^\gamma X^{0\sigma} + \alpha_2^\gamma X^{\bar\sigma 2} + Z^\gamma. \tag{24}$$

The operators $Z^{0\sigma(\bar\sigma 2)}$ are defined as orthogonal to the operators from the basic subspace [35–37]:

$$\langle\{Z^{0\sigma(\bar\sigma 2)}, X^{0\sigma(\bar\sigma 2)}\}\rangle = 0. \tag{25}$$

Thus, these equations (25) determine the projecting coefficients $\alpha_i^{0\sigma(\bar\sigma 2)}$ which are expressed in terms of mean values

$$\varphi_\sigma = \langle \xi_{\bar\sigma} X^{\bar\sigma 0}\rangle + \zeta\langle X^{\sigma 2}\xi_{\bar\sigma}^\dagger\rangle \tag{26}$$

and $A_{pq} = \langle X^{pp} + X^{qq}\rangle$.

This procedure leads to the Green's functions of the $\langle\langle Z^{0\sigma(\bar\sigma 2)} | X^{\sigma 0(2\bar\sigma)}\rangle\rangle$ type, and the similar procedure is applied with respect to the second time argument. As a result, we come to the Dyson equation for G_σ in a matrix representation

$$\hat G_\sigma = (1 - \hat G_0^\sigma \hat M_\sigma)^{-1} \hat G_0^\sigma, \tag{27}$$

where

$$\hat G_\sigma = 2\pi \begin{pmatrix} \langle\langle X^{0\sigma}|X^{\sigma 0}\rangle\rangle & \langle\langle X^{0\sigma}|X^{2\bar\sigma}\rangle\rangle \\ \langle\langle X^{\bar\sigma 2}|X^{\sigma 0}\rangle\rangle & \langle\langle X^{\bar\sigma 2}|X^{2\bar\sigma}\rangle\rangle \end{pmatrix}, \tag{28}$$

and the nonperturbed Green's function $\hat G_0^\sigma$ is

$$\hat G_0^\sigma = \frac{1}{D_\sigma} \begin{pmatrix} \omega - b_\sigma & -\zeta\frac{V_\sigma}{A_{2\bar\sigma}}\varphi_\sigma \\ -\zeta\frac{V_\sigma}{A_{0\sigma}}\varphi_\sigma & \omega - a_\sigma \end{pmatrix} \begin{pmatrix} A_{0\sigma} & 0 \\ 0 & A_{2\bar\sigma} \end{pmatrix}, \tag{29}$$

where

$$D_\sigma = (\omega - a_\sigma)(\omega - b_\sigma) - \frac{V_\sigma^2}{A_{0\sigma}A_{2\bar\sigma}}\varphi_\sigma^2, \tag{30}$$

$$a_\sigma = -\mu_\sigma + \frac{V_\sigma}{A_{0\sigma}}\varphi_\sigma, \quad b_\sigma = U - \mu_\sigma + \frac{V_\sigma}{A_{2\bar\sigma}}\varphi_\sigma. \tag{31}$$

The mass operator is equal to

$$\begin{aligned} \hat M_\sigma = 2\pi &\begin{pmatrix} A_{0\sigma}^{-1} & 0 \\ 0 & A_{2\bar\sigma}^{-1} \end{pmatrix} \\ &\times \begin{pmatrix} \langle\langle Z^{0\sigma}|Z^{\sigma 0}\rangle\rangle^{\rm ir} & \langle\langle Z^{0\sigma}|Z^{2\bar\sigma}\rangle\rangle^{\rm ir} \\ \langle\langle Z^{\bar\sigma 2}|Z^{\sigma 0}\rangle\rangle^{\rm ir} & \langle\langle Z^{\bar\sigma 2}|Z^{2\bar\sigma}\rangle\rangle^{\rm ir} \end{pmatrix} \begin{pmatrix} A_{0\sigma}^{-1} & 0 \\ 0 & A_{2\bar\sigma}^{-1} \end{pmatrix}, \end{aligned} \tag{32}$$

where the time correlation functions related by the spectral theorem to the Green's functions $\langle\langle Z|Z\rangle\rangle^{\rm ir}$ are calculated using procedure of different-time decoupling [45]. This procedure differs from the decoupling scheme proposed in [40] where the projecting technique and irreducible Green's functions were not used, and equations of motion were also written for the higher order Green's functions with the subsequent decoupling of operators from one side (with the same time). In our case, an independent averaging of the products of operators X and ξ (with different times) is performed in calculating $\langle\langle Z|Z\rangle\rangle^{\rm ir}$ functions. For example,

$$\begin{aligned} &\langle \xi_\sigma^\dagger(t)(X^{00} + X^{\sigma\sigma})_t (X^{00} + X^{\sigma\sigma})\xi_\sigma\rangle^{\rm ir} \\ &\qquad \approx \langle (X^{00} + X^{\sigma\sigma})_t (X^{00} + X^{\sigma\sigma})\rangle \langle \xi_\sigma^\dagger(t)\xi_\sigma\rangle. \end{aligned} \tag{33}$$

We calculate here the correlation functions for Hubbard operators in zero approximation

$$\langle (X^{00} + X^{\sigma\sigma})_t (X^{00} + X^{\sigma\sigma})\rangle \approx \langle (X^{00} + X^{\sigma\sigma})^2\rangle = A_{0\sigma}. \tag{34}$$

In this example, the following Green's function is reconstructed from the correlation functions using the spectral representation [35–37,44]:

$$I(\omega) = A_{0\sigma}\langle\langle\xi_\sigma|\xi_\sigma^\dagger\rangle\rangle_\omega^\xi = \frac{A_{0\sigma}}{2\pi V^2}J_\sigma(\omega). \tag{35}$$

Using the above procedure, we can obtain the final expressions for the total irreducible part:

$$\Xi_\sigma^{-1}(\omega) = \left[\frac{A_{0\sigma}}{\omega+\mu_\sigma-\Omega_\sigma(\omega)} + \frac{A_{2\bar\sigma}}{\omega+\mu_\sigma-U-\Omega_\sigma(\omega)}\right]^{-1} + \Omega_\sigma(\omega), \tag{36}$$

where

$$\Omega_\sigma(\omega) = J_\sigma(\omega) - \frac{R_\sigma(\omega)}{A_{0\sigma}A_{2\bar\sigma}} + \frac{V_\sigma\varphi_\sigma}{A_{0\sigma}A_{2\bar\sigma}}. \tag{37}$$

The function $R_\sigma(\omega)$ describes effects of the scattering on fluctuations related to the spin flip (sort change) and the creation and annihilation of holes, doubly occupied states. The full expression for R_σ in GH3 was given in [44] and in the simpler case of the standard Hubbard model in [36,37]. We called such an approximate scheme of calculating the total irreducible part the GH3 approximation.

The average values of the Hubbard operators are determined using the spectral representation of corresponding Green's functions. The particle density of states is calculated as an imaginary part of the interacting single-particle Green's function:

$$\rho_\sigma(\omega) = -\frac{1}{\pi}\lim_{\eta\to 0^+}\operatorname{Im}G_\sigma(\omega+\mathrm{i}\eta) \tag{38}$$

giving the concentration

$$n_\sigma = \int_{-\infty}^{+\infty}\frac{\rho_\sigma(\omega)\mathrm{d}\omega}{\mathrm{e}^{\beta\omega}+1}. \tag{39}$$

The Green's functions $\langle\langle\xi_\sigma|X^{pq}\rangle\rangle_\omega$ that are required to find φ_σ can be calculated from the exact relation

$$V_\sigma\langle\langle\xi_\sigma|X^{pq}\rangle\rangle_\omega = J_\sigma(\omega)\langle\langle a_\sigma|X^{pq}\rangle\rangle_\omega \tag{40}$$

that supplements the GH3 scheme and was derived in reference [44].

We consider below the special case of half-filling ($\mu_A = \mu_B = U/2$, $n_A = n_B = 1/2$), when due to the particle-hole symmetry we have:

$$\varphi_\sigma = 0, \quad R_\sigma(\omega) = -\frac{1}{2}J_{\bar\sigma}(\omega), \tag{41}$$

$$\Omega_\sigma(\omega) = J_\sigma(\omega) + 2J_{\bar\sigma}(\omega), \tag{42}$$

and

$$\Xi_\sigma^{-1}(\omega) = \omega - \frac{U^2}{4[\omega - J_\sigma(\omega) - 2J_{\bar\sigma}(\omega)]}. \tag{43}$$

In this case, the approximate solution of the single-site problem gives the usual Hubbard-III approximation for the standard Hubbard model ($t_A = t_B$, $J_A = J_B$).

In the case of the Falicov-Kimball model ($t_B = 0$, $J_B(\omega) = 0$) at half-filling, GH3 gives the following expression:

$$G_B(\omega) = \frac{\omega - 2J_A(\omega)}{\omega^2 - U^2/4 - 2\omega J_A(\omega)}, \tag{44}$$

where the coherent potential of itinerant particles (J_A) corresponding to the result of the alloy-analogy approximation is calculated exactly.

4 Other approximations to the asymmetric Hubbard model

4.1 Hubbard-I approximation

It was the Hubbard-I approximation [2] which in the simplest way described band forming in the Hubbard model with the strong on-site repulsion U. The total irreducible part in this approximation reads

$$\Xi_\sigma(\omega) = \frac{1-n_{\bar\sigma}}{\omega+\mu_\sigma} + \frac{n_{\bar\sigma}}{\omega+\mu_\sigma-U}. \tag{45}$$

It is well known that the Hubbard-I approximation gives an electron spectrum with the opened gap for any nonzero repulsion U (Fig. 1). Thus, this approximation cannot describe metal-insulator transitions. However, we consider it here to estimate its applicability at large U (see below) from a thermodynamic point of view.

The interacting single-site Green's function $G_\sigma(\omega)$ is calculated using the integration (17) with a noninteracting density of states $\rho_\sigma^0(\varepsilon)$. The band of particles of a given type (σ) depends here only on $\rho_\sigma^0(\varepsilon)$ and a concentration of particles of the opposite type, i.e., the transfer parameter $t_{\bar\sigma}$ does not have an effect on $G_\sigma(\omega)$.

In the large-U limit ($U \gg t_\sigma$), the density of states has the simple form

$$\rho_\sigma^{\mathrm{H-I}}(\omega) = \rho_\sigma^0\left(\frac{\omega+\mu_\sigma}{1-n_{\bar\sigma}}\right) + \rho_\sigma^0\left(\frac{\omega+\mu_\sigma-U}{n_{\bar\sigma}}\right). \tag{46}$$

Both spectral subbands are of the same height for any concentration values and are equal to $\rho_\sigma^0(\varepsilon)$ with the scaled bandwidth.

4.2 Alloy-analogy approximation

The system with one type of particles frozen on a lattice (for example when $t_B = 0$) can be mapped onto the problem of the electronic structure of simple binary alloys [17,46]. The alloy-analogy approximation is the single-site solution of the binary alloy problem within the coherent potential approximation [47] that is exact in infinite dimensions. Such a mapping onto the binary alloy is exact for the spinless Falicov-Kimball model with localized ions. Thus, the alloy-analogy approximation exactly describes the band formation by the particle hopping

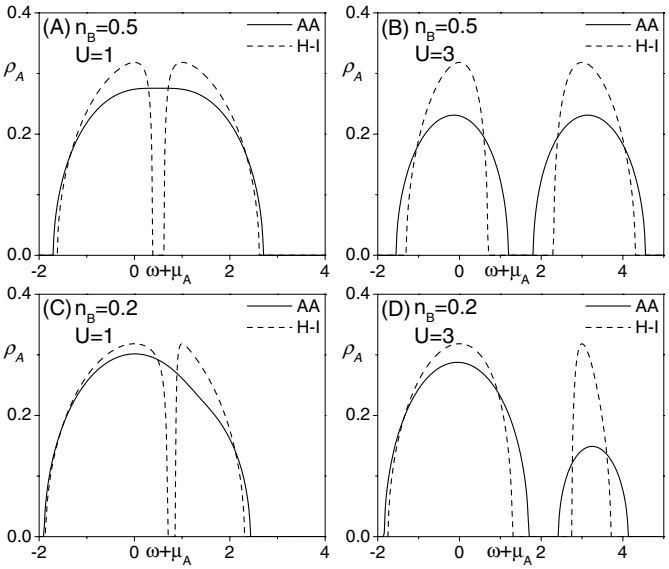

Fig. 1. Density of states ρ_A in the alloy-analogy (solid line) and Hubbard-I (dashed line) approximations on the Bethe lattice ($t_A = 1$) for various n_B and U.

(transfer) and the interaction with the localized particles. However, in the case of the asymmetric Hubbard model this approximation does not include an effect of the transfer of particles of another sort, like the Hubbard-I approximation.

The self-energy part for the Dyson equation in the alloy-analogy approximation reads

$$\Sigma_\sigma(\omega) = \frac{n_{\bar\sigma} U}{1 - G^\sigma_{ii}(\omega)(U - \Sigma_\sigma(\omega))}, \tag{47}$$

where the single-site Green's function:

$$G^\sigma_{ii}(\omega) = G_\sigma(\omega) = \frac{1 - n_{\bar\sigma}}{\omega + \mu_\sigma - J_\sigma(\omega)} + \frac{n_{\bar\sigma}}{\omega + \mu_\sigma - U - J_\sigma(\omega)}. \tag{48}$$

The Larkin irreducible part $\Xi^{-1}_\sigma = \omega + \mu_\sigma - \Sigma_\sigma$ is determined by the following expression

$$\Xi^{-1}_\sigma(\omega) = \left[\frac{1 - n_{\bar\sigma}}{\omega + \mu_\sigma - J_\sigma(\omega)} + \frac{n_{\bar\sigma}}{\omega + \mu_\sigma - U - J_\sigma(\omega)}\right]^{-1} + J_\sigma(\omega). \tag{49}$$

This approximation is obtained in our approach when the projecting constant φ_σ and the function $R_\sigma(\omega)$ in (37) are neglected.

To compare analytically results of the alloy-analogy approximation and the Hubbard-I approximation we can examine the equations in infinite-U limit. The self-consistency condition gives $J_\sigma = t^2_\sigma G_\sigma$ on the Bethe lattice with the semielliptic density of states

$$\rho^{\rm Bethe}_\sigma(\varepsilon) = \frac{1}{2\pi t^2_\sigma}\sqrt{4t^2_\sigma - \varepsilon^2}, \quad |\varepsilon| < 2t_\sigma. \tag{50}$$

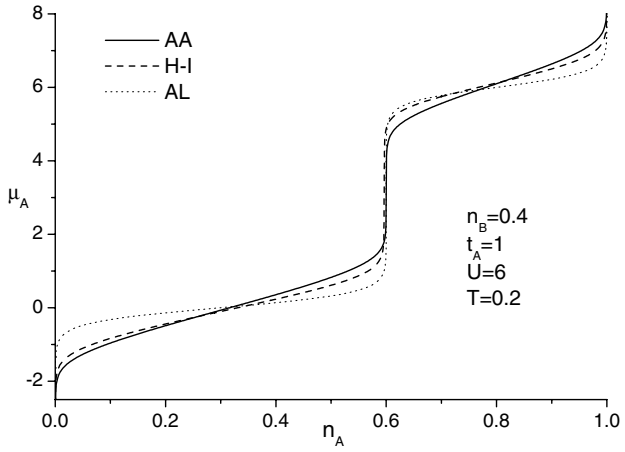

Fig. 2. Chemical potential as a function of the concentration in the alloy-analogy approximation (solid line) on the Bethe lattice compared to the Hubbard-I approximation (dashed line) and the atomic limit $t_\sigma \to 0$ (dotted line).

In this case, we have the following expression for the particle spectrum:

$$\rho^{\rm AA}_\sigma(\omega) = \frac{1}{2\pi t^2_\sigma}\sqrt{4t^2_\sigma(1 - n_{\bar\sigma}) - (\omega + \mu_\sigma)^2} \tag{51}$$

when $|\omega + \mu_\sigma| < 2t_\sigma\sqrt{1 - n_{\bar\sigma}}$ and zero otherwise. The height and width of this spectral band depend on the concentration $n_{\bar\sigma}$ and they are scaled proportionally to $\sqrt{1 - n_{\bar\sigma}}$ when $n_{\bar\sigma}$ changes. Therefore, the bandwidth of the subbands (for finite U) is wider in the alloy-analogy approximation at half-filling Figures 1A, 1C as well as off half-filling Figures 1B, 1D. In Figure 2, the effect of wider subbands is illustrated by the dependence of the chemical potential μ_A on the concentration n_A calculated using the particle density of states (38).

5 Analytic properties at Mott transition

We consider here the metal-insulator transition at half-filling. It is known that there is a range of the interaction strength ($U_{\rm c1}(T) < U < U_{\rm c2}(T)$) where metallic and insulating solutions coexist for the Hubbard model at low temperature in paramagnetic state [11,31,33] leading to the first-order transition. At zero temperature when the transition is approached from the metallic side, $\mathrm{Im}\,\Sigma_\sigma(0) = 0$ and the real part has the following low-frequency form [11]

$$\mathrm{Re}\,\Sigma_\sigma(\omega + \mathrm{i}0^+) = U/2 + (1 - 1/Z)\omega + \mathrm{O}(\omega^3) \tag{52}$$

corresponding to Fermi liquid behaviour, where Z defines the quasiparticle weight. Such self-energy gives particle densities of states with a quasiparticle peak at the Fermi-level that has the same height for different U up to the critical value $U_{\rm c} = U_{\rm c2}$ [27]. The gap opens when $Z \to 0$ and in the metallic phase the relation $G_\sigma(0)J_\sigma(0) = -1$ is satisfied.

However, for finite temperatures the Fermi-liquid state breaks near the transition point $U_{\rm c}$. Therefore, $\Sigma_\sigma(0)$ has

a nonzero imaginary part [31], and the limit $Z \to 0$ cannot indicate the transition. In this case, the density of states at Fermi-level continuously tends to zero. At high enough temperatures, the Mott transition turns into a smooth crossover from a bad metal to a bad insulator [23,48]. Another limit of the asymmetric Hubbard model (the Falicov-Kimball model) at half-filling does not have a central quasiparticle peak for finite temperature in the spectrum [20,22].

The alloy-analogy, Hubbard-III and GH3 approximations cannot describe the Fermi liquid behaviour at half-filling. Therefore, the set of equations in these approximations cannot give a solution describing gap opening with quasiparticle features (U_{c2}) and there is no coexisting solutions. The processes taken into account give the only solution corresponding to U_{c1} for the Hubbard model at low temperature. Hence, the approximations can be applied to the investigation of high temperature properties of the system when the quasiparticle features are absent. In this case, the gap opens continuously when the critical energy U is approached from the metallic side.

Hereafter the term "continuous transition" means not a thermodynamic phase transition. It concerns gap opening in the spectrum.

To investigate the continuous transition in the asymmetric Hubbard model, we derive some properties following from the particle hole-symmetry.

5.1 Exact relations between $G_\sigma(0)$, $J_\sigma(0)$ and $\Xi_\sigma(0)$ at continuous transition at half-filling

In the case of the symmetric noninteracting density of states

$$\rho^0_\sigma(\varepsilon) = \rho^0_\sigma(-\varepsilon) \tag{53}$$

leading to the particle-hole symmetry with the properties

$$G_\sigma(\omega) = -G_\sigma(-\omega), \quad J_\sigma(\omega) = -J_\sigma(-\omega) \tag{54}$$

of the single-particle Green's function and the coherent potential at half-filling, the following relations can be proven

$$\lim_{U\to U_c^-} \frac{J_\sigma(0)}{G_\sigma(0)} = \int_{-\infty}^{+\infty} \varepsilon^2 \rho^0_\sigma(\varepsilon)\mathrm{d}\varepsilon, \tag{55}$$

$$\lim_{U\to U_c^-} G_\sigma(0)\Xi_\sigma^{-1}(0) = 1 \tag{56}$$

which take place at zero frequency when the continuous metal-insulator transition is approached from below (when the gap opens in the particle spectrum at $\omega = 0$).

Proof. Let us consider general properties of the Green's functions (G_σ, J_σ) and the total irreducible part Ξ_σ following from (54) at zero frequency. These functions can be written in the Lehmann representation

$$F(\omega) = -\frac{1}{\pi} \lim_{\eta\to 0^+} \int_{-\infty}^{+\infty} \frac{\operatorname{Im} F(\omega' + \mathrm{i}\eta)\mathrm{d}\omega'}{\omega - \omega'}. \tag{57}$$

This representation shows that due to the symmetry (54) the functions at $\omega = 0$ are pure imaginary, and there are three possible cases: (i) $F(0) = 0$; (ii) $\operatorname{Re} F(0) = 0$, $\operatorname{Im} F(0) = \text{const}$; (iii) the pole of $F(\omega)$ in the real axis at $\omega = 0$.

An imaginary part of $G_\sigma(\omega \pm \mathrm{i}0^+)$ defines the particle spectrum (38). When the gap continuously opens the single-particle Green's function tends to zero at $\omega = 0$. It means that $\Xi_\sigma^{-1}(0)$ is pure imaginary

$$\lim_{\eta\to 0^+} \Xi_\sigma^{-1}(\pm\mathrm{i}\eta) = \pm\mathrm{i}B_\sigma, \quad B_\sigma > 0, \tag{58}$$

and the gap opens (in the non-Fermi liquid state) only when B_σ continuously increases up to infinity, i.e., the self-energy diverges [11,31,49].

The coherent potential can be expressed from (14) as a function of G_σ and the total irreducible part Ξ_σ:

$$\frac{J_\sigma}{G_\sigma} = \frac{\Xi_\sigma^{-1} G_\sigma - 1}{G_\sigma^2}. \tag{59}$$

Using that the noninteracting density of states is symmetric (53) and normalized

$$\int_{-\infty}^{+\infty} \rho^0_\sigma(\varepsilon)\mathrm{d}\varepsilon = 1, \tag{60}$$

we have:

$$G_\sigma = \mp\mathrm{i}B_\sigma \int_{-\infty}^{+\infty} \frac{\rho^0_\sigma(\varepsilon)\mathrm{d}\varepsilon}{\varepsilon^2 + B_\sigma^2}, \tag{61}$$

and

$$G_\sigma J_\sigma = \Xi_\sigma^{-1} G_\sigma - 1 = -\int_{-\infty}^{+\infty} \frac{\varepsilon^2 \rho^0_\sigma(\varepsilon)\mathrm{d}\varepsilon}{\varepsilon^2 + B_\sigma^2} \tag{62}$$

from (17).

When the critical value U_c is approached from below, the limit $B_\sigma \to +\infty$ should be considered. In this limit, inserting (61) and (62) into (59) leads to the result (55).

To prove (56), we consider three different cases depending on behaviour of the function $\rho^0_\sigma(\varepsilon)$ at large energies.

1. If an average kinetic energy per particle is finite, the limit
$$\lim_{\varepsilon\to\infty} \varepsilon^2 \rho^0_\sigma(\varepsilon) = 0 \tag{63}$$
is satisfied giving the dependence $G_\sigma J_\sigma \sim B_\sigma^{-2}$ (62) at large B_σ. It means that $J_\sigma(0) \to 0$ at the transition.
2. When the density of states has the power-law tails of order ε^{-2}
$$\lim_{\varepsilon\to\infty} \varepsilon^2 \rho^0_\sigma(\varepsilon) = \text{const} > 0, \tag{64}$$
the limiting behaviour $G_\sigma J_\sigma \sim B_\sigma^{-1}$ is realized at the transition. In this case a finite imaginary part of $J_\sigma(0)$ remains when $B_\sigma \to \infty$, and the ratio $J_\sigma(0)/G_\sigma(0)$ tends to infinity (55).
An example of such a function is the Lorentzian density of states describing a lattice with long-range hopping along coordinate axes
$$\rho^0_\sigma(\varepsilon) = \frac{t_\sigma}{\pi(\varepsilon^2 + t_\sigma^2)}. \tag{65}$$

This density of states always gives a constant value for the coherent potential:

$$\lim_{\eta\to 0^+} J_\sigma(\omega \pm \mathrm{i}\eta) = \mp \mathrm{i}t_\sigma. \tag{66}$$

3. The last case is when $\rho^0_\sigma(\varepsilon) \sim \varepsilon^{-n}$, $n \in (1,2)$ at large energy ε. The integrals (60) and (62) are convergent only when $n > 1$. Such power-law tails give the following limiting behaviour $G_\sigma J_\sigma \sim 1/(B_\sigma)^{n-1}$ and $J_\sigma \sim (B_\sigma)^{2-n}$ at large B_σ.

All these cases show that the relation

$$\lim_{U\to U_{\mathrm{c}}^-} G_\sigma(0) J_\sigma(0) = -0 \tag{67}$$

is satisfied proving the relation (56).

5.2 Critical value U_{c} for the Mott transition within GH3 approximation with symmetric density of states

Due to (55), we have

$$J_\sigma(0) = W_\sigma^2 G_\sigma(0)/4 \tag{68}$$

at the Mott transition, where W_σ is the effective half-bandwidth of the unperturbed density of states ρ^0_σ:

$$W_\sigma = 2\left(\int_{-\infty}^{+\infty} \varepsilon^2 \rho^0_\sigma(\varepsilon)\mathrm{d}\varepsilon\right)^{1/2}. \tag{69}$$

Due to $G_\sigma(0)\Xi_\sigma^{-1}(0) = 1$ (56) at the transition, inserting (68) into (43) yields a set of equations:

$$\lim_{U\to U_{\mathrm{c}}^-} \frac{U^2 G_A(0)}{W_A^2 G_A(0) + 2W_B^2 G_B(0)} = 1, \tag{70}$$

$$\lim_{U\to U_{\mathrm{c}}^-} \frac{U^2 G_B(0)}{W_B^2 G_B(0) + 2W_A^2 G_A(0)} = 1. \tag{71}$$

The ratio

$$\eta = \lim_{U\to U_{\mathrm{c}}^-} \frac{G_A(0)}{G_B(0)} \tag{72}$$

is excluded from the set of equations, and we have the following equation for U_{c}

$$U_{\mathrm{c}}^4 - (W_A^2 + W_B^2)U_{\mathrm{c}}^2 - 3W_A^2 W_B^2 = 0 \tag{73}$$

with the solution

$$U_{\mathrm{c}} = \sqrt{\frac{W_A^2 + W_B^2 + (W_A^4 + W_B^4 + 14W_A^2W_B^2)^{1/2}}{2}}. \tag{74}$$

If we put $W_B = 0$, the expression (74) describes the Mott-type transition in the alloy-analogy approximation (which is exact for the Falicov-Kimball model) giving well known results: $U_{\mathrm{c}} = W_A = 2t_A$ for the Bethe lattice and $U_{\mathrm{c}} = \sqrt{2}t_A$ for the hypercubic lattice with

$$\rho^{\mathrm{hyp}}_\sigma(\varepsilon) = \frac{1}{t_\sigma\sqrt{\pi}} \exp\left(-\frac{\varepsilon^2}{t_\sigma^2}\right). \tag{75}$$

In the case of the standard Hubbard model ($W_A = W_B = W$), we have $U_{\mathrm{c}} = \sqrt{3}W$ corresponding to the Hubbard-III approximation at half-filling (see Refs. [11,16] for reviews of the limits: the standard Hubbard model and the Falicov-Kimball model).

6 Results and discussion

There are two different pairs of parameters (n_A, μ_A and n_B, μ_B) in the asymmetric Hubbard model which have to be determined from the thermodynamic equilibrium. Thus, various thermodynamic regimes may be considered when different pairs of the thermodynamic parameters are fixed: (μ_A, μ_B), (μ_A, n_B), (n_A, n_B), etc. It is known that there are possible phase separations at low temperatures in the case of the Falicov-Kimball model [35,50,51] and in the general case of the asymmetric Hubbard model [7]. Besides the segregated phases, the long-range antiferromagnetic-type ordering is possible at low temperatures [3].

Since the investigation of the asymmetric Hubbard model is a very complicated problem, we restrict our analysis to temperatures higher than the critical temperatures of thermodynamic instabilities. Thus, the problem is reduced to the investigation of a band structure and metal-insulator transitions at constant particle concentrations.

The simplest approximations such as the Hubbard-I and alloy-analogy approximations describe the band of particles generated by the particle hopping and the interaction with particles of another sort. These approximations can describe an effect of the transfer parameter t_A on the spectrum $\rho_B(\omega)$ only via the concentration n_A, i.e., when the concentrations are fixed the band $\rho_B(\omega)$ does not depend on t_A, and for $t_A \neq 0$, $t_B = 0$ the approximate spectrum $\rho_B(\omega)$ has a form of two delta-peaks. However, the alloy-analogy approximation is exact for itinerant particles in the Falicov-Kimball model when another sort of particles is localized. Thus, this approximation can give simple reasonable results for dependence $\mu_\sigma = \mu_\sigma(n_\sigma, n_{\bar\sigma})$ in the limit of small values of $n_{\bar\sigma}$ or $t_{\bar\sigma}$.

In the alloy-analogy approximation, the critical value of U for the band $\rho_\sigma(\omega)$ depends only on t_σ and $n_{\bar\sigma}$. Hence, the critical repulsion depends on a sort of particles ($U_{\mathrm{c}} \to U_{\mathrm{c}}^\sigma$). Even at half-filling where $U_{\mathrm{c}}^\sigma = W_\sigma$ we have $U_{\mathrm{c}}^A \neq U_{\mathrm{c}}^B$ when $t_A \neq t_B$. Such a behaviour is similar to orbital-selective Mott transitions in the two-band Hubbard model (for example see [52,53]). However, in this case, such a result is rather an effect of the approximation because in the approximation of a higher order (GH3), U_{c} is given by the equation (74) and $U_{\mathrm{c}}^A = U_{\mathrm{c}}^B$.

The generalization of the Hubbard-III approximation (GH3) gives the total irreducible part and the single-site Green's function as a functional of the coherent potentials of both sorts of particles (see Eqs. (36)–(41)). Unlike the alloy-analogy approximation, GH3 described broadening of the band by the interaction with particles of another sort, and it gives a finite bandwidth for localized particles in the Falicov-Kimball model. In general, the spectral density in the GH3 approximation is temperature dependent; such an approximation can be applied for systems with different values of the transfer parameters (both $t_A = t_B$ and $t_A \neq t_B$) and various particle concentrations. However, the approximation has some restrictions. In reference [44], GH3 was applied to the calculation of the chemical potential and spectrum of localized particles in the Falicov-Kimball model. It was shown that the approximation gives

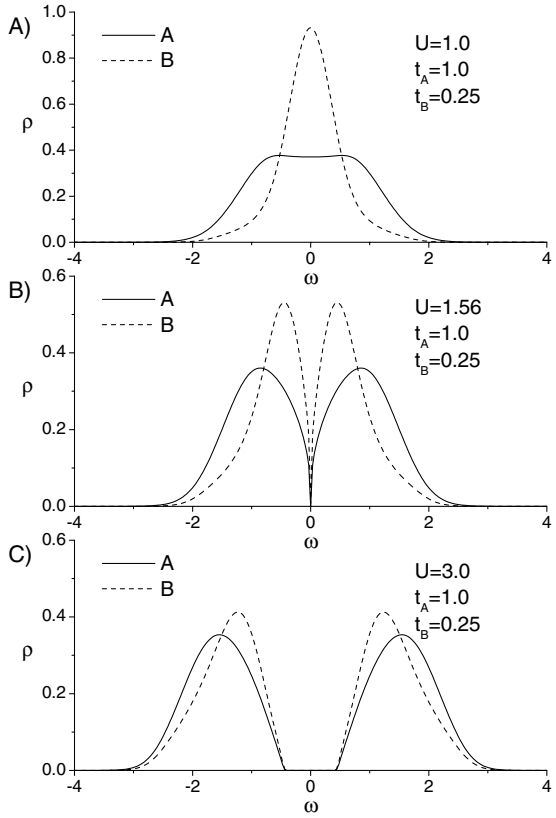

Fig. 3. Densities of states of particles in the asymmetric Hubbard model within the GH3 approximation for various values of U at half-filling on the hypercubic lattice.

better results when the concentration of itinerant particles is low.

In the symmetric case of half-filling the approximate density of states is independent of temperature (Fig. 3), because the chemical potentials do not depend on temperature and the projecting coefficients and coefficients of the integral terms in $R_\sigma(\omega)$ (for example see [44]) are equal to zero. In the Falicov-Kimball model at half-filling, the approximation (44) can be compared with the exact results [20,22]. We find that the approximation gives a better correspondence with the exact curves at high temperatures, and the best correspondence is for high U when the exact results weakly depend on temperature [44]. Figure 3A shows that the density of states of heavy particles B (the case of $t_B < t_A$) is in the form of a single peak for the low interaction U. For the higher interaction strength Figures 3B, 3C, the spectrum $\rho_B(\omega)$ has two subbands with peaks which are closer to the centre ($\omega = 0$) than in the spectrum of light particles $\rho_A(\omega)$. This agrees with the results obtained for the Falicov-Kimball model when $t_B = 0$.

The particle-hole symmetry at half-filling simplifies the investigation of the problem. Such symmetry requires the divergence $(1/\omega)$ of the self-energy at zero frequency when the gap opens continuously [31,49]. Thus, the limit behaviour (55), (56) of the Green's function and the coherent potential at the transition (gap opening) is proven analytically, which allows us to perform some analytic analysis.

In Figure 3, the transition with the opening gap is illustrated for the asymmetric Hubbard model within the GH3 approximation. There are only continuous transitions. This agrees with the continuous metal-insulator reconstruction of the spectrum at high temperatures for the standard Hubbard model [26,31], and the fact that in the case of the Falicov-Kimball model the gap opens continuously with increasing U [16]. The spectra of both types of particles have the same bandwidth in the approximation. This is because it cannot describe tails of the subbands that raise with the temperature increase as it is for localized particles in the Falicov-Kimball model [20,22].

Since the effect of temperature broadening of the band and quasiparticle features are not captured, it can be predicted that the approximation underestimate the critical value U_c. For the Falicov-Kimball model our method gives the exact value for $U_c = W_A$ ($W_B = 0$) because it gives the exact density of states of mobile particles. For the localized particles, it was shown in [44] that the expression (44) can describe density of states $\rho_B(\omega)$ correctly for large values of U and high temperature. In the opposite limit of the standard Hubbard model, our approximation gives large underestimation of U_c. In the GH3 approximation, U_c is equal to $\sqrt{3}W \approx 1.73W$. However, it is known that U_c should be dependent on temperature and its value is around $(2.4-2.5)W$ for high temperatures [26,31]. Thus, our method gives better results near the Falicov-Kimball limit, and it can be used as an approximation considering the asymmetric Hubbard model as the extended Falicov-Kimball model. For the better description of the standard Hubbard model and quasiparticle features, further improvement is required in the decoupling scheme. For example, it can be achieved by writing higher order equations of motion for operators from one side of the Green's functions.

The energy band edges as a function of U within various approximations on the Bethe lattice are displayed in Figure 4. In the Hubbard-I approximation the spectrum is always split having the gap and two subbands. The alloy-analogy approximation is exact for the band of itinerant particles when $t_B = 0$ and it gives the critical interaction constant $U_c^{AA} = 2t_A$. The GH3 approximation describes the band which is broadened by simultaneous contribution of the hopping of both types of particles, and the critical value $U_c > U_c^{AA}$. Because of the particle-hole symmetry at half-filling the critical value U_c can be calculated analytically in the GH3 approximation and it is given by the expression (74), see Figure 5. The obtained result can be applied to various lattices (hypercubic, Bethe, etc.) when the energy is scaled in the following way:

$$U_c^* = \frac{U_c}{W_A} = \frac{U_c}{2}\left(\int_{-\infty}^{+\infty} \varepsilon^2 \rho_A^0(\varepsilon)\mathrm{d}\varepsilon\right)^{-1/2}. \qquad (76)$$

It is common practice to normalize U by a typical kinetic energy (W_A) investigating the Mott transition in the standard Hubbard model [11]. In this case, such normalization shows that the scaled result does not depend on a form

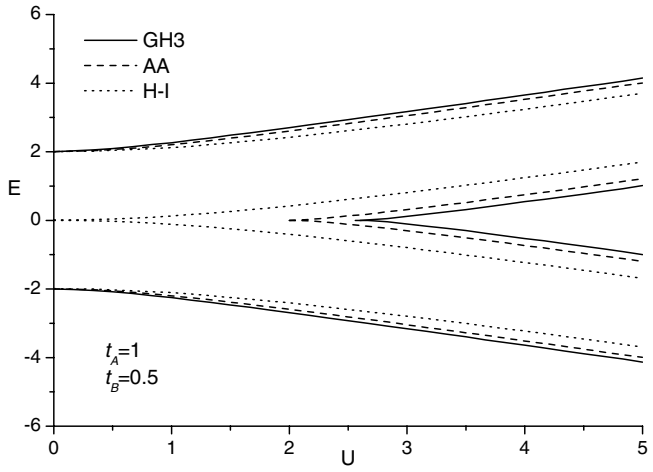

Fig. 4. Dependence of the energy band edges on the repulsion strength U at half-filling $n_A = n_B = 1/2$ on the Bethe lattice: $t_A = 1$, $t_B = 0.5$. The solid line is the GH3 approximation, the dashed and dotted lines are the alloy-analogy and Hubbard-I approximations, respectively.

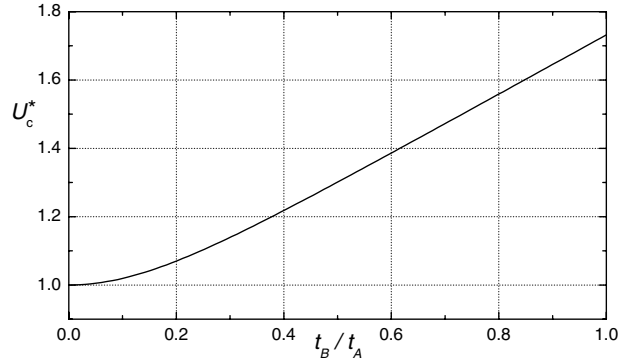

Fig. 5. Scaled critical value $U_c^* = U_c/W_A$ (76) as a function of t_B/t_A within the GH3 approximation at half-filling.

of the noninteracting density of states. For the Lorentzian density of states (65) with long-range hopping an average kinetic energy per particle tends to infinity ($W_A \to \infty$), and as it was noted in reference [54], this requires an infinite interaction U to drive the system insulating.

7 Conclusions

The generalization of the Hubbard-III approximation is obtained for the asymmetric Hubbard model using the equation of motion approach. This method combines in a unified framework the description of the band structure of the Falicov-Kimball model and the standard Hubbard model. In general, the approach can be used to calculate the particle spectrum in the system with the different particle concentrations at various temperatures, and it gives nontrivial results for the spectrum of localized particles in the Falicov-Kimball model.

Our method gives better results around the Falicov-Kimball limit. Taking into account the restrictions of approximations, GH3 can be applied to the asymmetric Hubbard model when particles of one type have the effective mass much larger than particles of other type ($t_B \ll t_A$).

The self-consistency condition connecting mutually the single-site Green's function and coherent potential gives the simple result (55) when the metal-insulator transition (gap opening) occurs at half-filling on the lattice with a symmetric noninteracting density of states. As a result, we have the expression (74) in the GH3 approximation for the critical value of U that provides a universal solution for various lattices and different values of the hopping integrals.

Since the approximation has various restrictions, to describe the system at half-filling with the proper temperature dependence or quasiparticle peak, the approach needs further improvement in calculating the mass operator by including higher order corrections in calculating bosonic Green's functions or/and by writing higher order equations of motion for operators with the same time (from one side of the Green's functions).

References

1. L.M. Falicov, J.C. Kimball, Phys. Rev. Lett. **22**, 997 (1969)
2. J. Hubbard, Proc. R. Soc. London, Ser. A **276**, 238 (1963)
3. A.N. Kocharian, G.R. Reich, J. Appl. Phys. **76**, 6127 (1994)
4. C.D. Batista, Phys. Rev. Lett. **89**, 166403 (2002)
5. A.N. Kocharian, G.R. Reich, Physica B **206-207**, 719 (1995)
6. C. Gruber, R. Kotecký, D. Ueltschi, J. Phys. A: Math. Gen. **33**, 7857 (2000)
7. D. Ueltschi, J. Stat. Phys. **116**, 681 (2004)
8. G. Fáth, Z. Domański, R. Lemański, Phys. Rev. B **52**, 13910 (1995)
9. C.A. Macedo, A.M.C. de Souza, Phys. Rev. B **65**, 153109 (2002)
10. W. Metzner, D. Vollhardt, Phys. Rev. Lett. **62**, 324 (1989)
11. A. Georges, G. Kotliar, W. Krauth, M.J. Rozenberg, Rev. Mod. Phys. **68**, 13 (1996)
12. E. Müller-Hartmann, Z. Phys. B **74**, 507 (1989)
13. V.I. Anisimov, A.I. Poteryaev, M.A. Korotin, A.O. Anokhin, G. Kotliar, J. Phys.: Condens. Matter **9**, 7359 (1997)
14. K. Held, I.A. Nekrasov, G. Keller, V. Eyert, N. Blümer, A.K. McMahan, R.T. Scalettar, T. Pruschke, V.I. Anisimov, D. Vollhardt, Psi-k Newsletter **56**, 65 (2003)
15. A. Georges, e-print `arXiv:cond-mat/0403123` (2004)
16. J.K. Freericks, V. Zlatić, Rev. Mod. Phys. **75**, 1333 (2003)
17. U. Brandt, C. Mielsch, Z. Phys. B **75**, 365 (1989)
18. U. Brandt, C. Mielsch, Z. Phys. B **79**, 295 (1990)
19. U. Brandt, C. Mielsch, Z. Phys. B **82**, 37 (1991)
20. U. Brandt, M.P. Urbanek, Z. Phys. B **89**, 297 (1992)
21. V. Zlatić, J.K. Freericks, R. Lemański, G. Czycholl, Phil. Mag. B **81**, 1443 (2001)
22. J.K. Freericks, V.M. Turkowski, V. Zlatić, Phys. Rev. B **71**, 115111 (2005)
23. D.E. Logan, P. Nozières, Philos. Trans. R. Soc. London, Ser. A **356**, 249 (1998)

24. R.M. Noack, F. Gebhard, Phys. Rev. Lett. **82**, 1915 (1999)
25. W. Krauth, Phys. Rev. B **62**, 6860 (2000)
26. J. Schlipf, M. Jarrell, P.G.J. van Dongen, N. Blümer, S. Kehrein, T. Pruschke, D. Vollhardt, Phys. Rev. Lett. **82**, 4890 (1999)
27. R. Bulla, Phys. Rev. Lett. **83**, 136 (1999)
28. M.J. Rozenberg, R. Chitra, G. Kotliar, Phys. Rev. Lett. **83**, 3498 (1999)
29. R. Bulla, M. Potthoff, Eur. Phys. J. B **13**, 257 (2000)
30. Y. Ōno, R. Bulla, A.C. Hewson, M. Potthoff, Eur. Phys. J. B **22**, 283 (2001)
31. R. Bulla, T.A. Costi, D. Vollhardt, Phys. Rev. B **64**, 045103 (2001)
32. M.P. Eastwood, F. Gebhard, E. Kalinowski, S. Nishimoto, R.M. Noack, Eur. Phys. J. B **35**, 155 (2003)
33. D. Vollhardt, K. Held, G. Keller, R. Bulla, T. Pruschke, I.A. Nekrasov, V.I. Anisimov, J. Phys. Soc. Jpn **74**, 136 (2005)
34. G. Kotliar, J. Phys. Soc. Jpn **74**, 147 (2005)
35. I.V. Stasyuk, O.B. Hera, Condens. Matter Phys. **6**, 127 (2003)
36. I.V. Stasyuk, Condens. Matter Phys. **3**, 437 (2000)
37. I.V. Stasyuk, A.M. Shvaika, Ukr. J. Phys. **47**, 975 (2002)
38. T. Herrmann, W. Nolting, Phys. Rev. B **53**, 10579 (1996)
39. J. Hubbard, Proc. R. Soc. London, Ser. A **281**, 401 (1964)
40. H.O. Jeschke, G. Kotliar, Phys. Rev. B **71**, 085103 (2005)
41. A.I. Larkin, Zh. Eksp. Teor. Fiz. **37**, 264 (1959); A.I. Larkin, Sov. Phys. JETP **10**, 186 (1960)
42. A.M. Shvaika, Phys. Rev. B **67**, 075101 (2003)
43. W. Metzner, Phys. Rev. B **43**, 8549 (1991)
44. I.V. Stasyuk, O.B. Hera, Phys. Rev. B **72**, 045134 (2005)
45. N.M. Plakida, Phys. Lett. A **43**, 481 (1973)
46. J.K. Freericks, L.M. Falicov, Phys. Rev. B **41**, 2163 (1990)
47. B. Velický, S. Kirkpatrick, H. Ehrenreich, Phys. Rev. **175**, 747 (1968)
48. M.J. Rozenberg, G. Kotliar, X.Y. Zhang, Phys. Rev. B **49**, 10181 (1994)
49. C. Gros, Phys. Rev. B **50**, 7295 (1994)
50. J.K. Freericks, C. Gruber, N. Macris, Phys. Rev. B **60**, 1617 (1999)
51. B.M. Letfulov, Eur. Phys. J. B **11**, 423 (1999)
52. C. Knecht, N. Blümer, P.G.J. van Dongen, Phys. Rev. B **72**, 081103 (2005)
53. A. Liebsch, Phys. Rev. Lett. **95**, 116402 (2005)
54. A. Georges, G. Kotliar, Q. Si, Int. J. Mod. Phys. B **6**, 705 (1992)